CHINESE JOURNAL OF ANALYTICAL CHEMISTRY
Volume 46, Issue 12, December 2018
Online English edition of the Chinese language journal

Available online at www.sciencedirect.com
ScienceDirect

Cite this article as: Chinese J. Anal. Chem., 2018, 46(12): 1878–1885

RESEARCH PAPER

Research on Dispersive Detection Technology Based on Digital Micromirror Device by Atomic Fluorescence Spectrometry

TAO Chen[1], LI Chun-Sheng[1,*], WANG Hong-Xia[1], ZHANG Ya-Ru[1], ZHAO Cheng-Wei[1], ZHOU Zhi-Heng[2], MA Zhen-Yu[3], TIAN Di[1,*]

[1] College of Instrumentation & Electrical Engineering, Jilin University, Changchun 130023, China
[2] Beijing Bohui Innovation Optoelectronic Technology Co., Ltd, Beijing 102206, China
[3] Grating Technology Laboratory, Changchun Institute of Optics and Fine Mechanics and Physics, Chinese Academy of Sciences, Changchun 130033, China

Abstract: A ultraviolet (UV) digital micromirror spectrometer using a digital micromirror device (DMD) as a spatial light modulator, a grating as a spectroscope and a photomultiplier tube (PMT) as a detector, was specially designed for dispersive hydride generation atomic fluorescence spectrometry (HG-AFS). To improve the detection ability of the UV digital micromirror spectrometer for weak fluorescence signals at 180–320 nm, a high UV transmittance DMD was used and the signal acquisition system was improved, and the control parameters of DMD and PMT negative high voltage were optimized. The feasibility of the spectrometer was demonstrated with standard sample analyzing of As, Sb, Bi, and Hg, the emission and atomic fluorescence spectra were obtained, and the scattering interference caused by the light source was discussed. The results showed that the UV digital micromirror spectrometer had a preliminary ability for the excitation fluorescence analysis by HG-AFS. In addition, due to no macroscopic moving parts, the UV digital micromirror spectrometer had simple construction and fast analysis speed (0.848 s per spectrum scan).

Key Words: Hydride generation atomic fluorescence spectrometry; Dispersive detection; Digital micro-mirror device; UV digital micromirror spectrometer

1 Introduction

Hydride generation-atomic fluorescence spectrometry (HG-AFS) has been widely used in the detection and analysis of heavy metals in food, agricultural products and other fields[1–4], especially for trace and ultra-trace detection of As, Sb, Bi and other elements[5–7]. At present, the relevant method standards in Europe and the United States have some restrictions on HG-AFS. For example, the US Environmental Protection Agency standard (EPA Method 1631, Revision E)[8] only admit the method for detection of Hg by cold atomic fluorescence spectrometry. One of the main reasons is that the non-dispersive detection systems of HG-AFS fail to recognize and calibrate for the spectral and scattering interference. Therefore, there is a necessary for an effective dispersive detection system to solve the problem of scattered interference.

The excitation fluorescence of HG-AFS is mainly distributed in 180–320 nm, which requires the dispersion detection method with high sensitivity and response speed. Current common methods such as electro-mechanical scanning grating devices need high rotational precision and a long detection time[9]; monochromator is not suitable for the rapid detection of different elements[10]; and charge coupled devices (CCD) spectrometer is hard to meet the requirements of high sensitivity for weak atomic fluorescence[11]. In recent years, digital micro mirror device (DMD) has brought new

Received 22 July 2018; accepted 8 October 2018
*Corresponding author. E-mail: tiandi@jlu.edu.cn; lics@jlu.edu.cn
This work was supported by the National Key Research and Development Program of China (No. 2016YFF0103303).

DOI: 10.1016/S1872-2040(18)61128-4

possibilities for AFS dispersion detection. DMD is a kind of micro-electro-mechanical system and commonly used as the core component of digital optical processing technology. Each piece of DMD chip integrates nearly one million micron-sized micromirrors. As an example by 0.7 XGA DMD, it has 1024×768 micro reflections, and each micromirror has a width of only 13.68 μm and an interval of 0.1 μm, what's more, it can be rotated in microsecond control speed (up to 23600 fps). The working angle of the DMD can be reversed to +12 degree and –12 degree. The +12 degree micro-mirror can be set to reflect the incident light onto the photodetector, and the state of the direction is "on state"; the –12 degree micro-mirror reflects the incident light as the unwanted spectrum signal, and the state in this direction is the "off state". This spectrum analysis technique using DMD as spatial light modulator has the characteristics of fast response, no macroscopic moving parts and high stability. The first use of a DMD as a light modulator in a visible spectrometer was published by Wagner et al. in 1995[12]. Since then, DMD has also been used in Raman spectroscopy[13], Hadamard transform near-infrared spectrometers[14–16], flame atomic absorption spectrometers[17] and other analytical instruments. Texas Instruments (TI) has also been introduced NIRscan and NIRscan nano near-infrared spectrometer.

Although DMD was proven to be a promising spatial light modulator (SLM) for the spectral analysis of long wavelength UV range, the most common type of borosilicate glass used in the commercial UV DMD (TI, DLP® 0.7 XGA UV DMD) had a 0% optical transmission below 280 nm[18], and the further application of DMD in HG-AFS and other UV spectroscopy was limited. In this study, an UV digital micromirror spectrometer contained a high UV transmittance DMD (made of Corning HPFS® 7980 fused quartz), a grating and a photomultiplier tube (PMT) was specially designed for dispersive HG-AFS. With the improvement of the signal acquisition system and under the optimized control parameters of DMD and PMT negative high voltage, the possible scattering interference of light source was investigated, and the emission and excitation fluorescence lines of As, Sb, Bi and Hg were analyzed as well.

2 System structure

2.1 UV digital micromirror spectrometer

The basic structure of the UV digital micromirror spectrometer is shown in Fig.1A. After the hydride reaction, the sample was atomized and excited in the atomizer. The fluorescence signal was collected though a silt (800 μm height, 100 μm width), then dispersed by a concave flat field grating (1000 grooves/mm grating, f = 30 mm, spectral region from 180–320 nm, Changchun Institute of Optics, Fine Mechanics and Physics, China), and sent onto the high UV transmittance DMD (modified by the TI 0.7 XGA DMD, provided by Changchun Institute of Optics, Fine Mechanics and Physics, Chinese Academy of Sciences). The DMD control commands were directly loaded into the chipset consist of APPSFPGA, DDC4100 and DAD2000 which in the Wintech 4100 DMD controller (Wintech Technology Development Co., Ltd, Beijing, China). The fluorescence was reflected to the mirror, and finally sent to the PMT (R7154, 160–320 nm, Hamamatsu, Japan), transmitted back to the host computer by the signal acquisition system. Figure 1B is the physical map of the UV digital micromirror spectrometer, in which a hood is used to avoid ambient light effects.

2.2 Signal acquisition system

As shown in Fig.2, the PMT was combined with a high-precision (18 bit) and high-speed (5 MHz sampling rate) analog to digital converter (ADC), and an acquisition circuit was designed to obtain larger measurement range and a better SNR. To improve the acquiring capability of weak fluorescence signal, an alternating current (AC) synchronization signal was induced to eliminate interference of power frequency, and a low voltage differential signaling (LVDS) interface was used to achieve high connection transmission speed (400 Mbit s^{-1}).

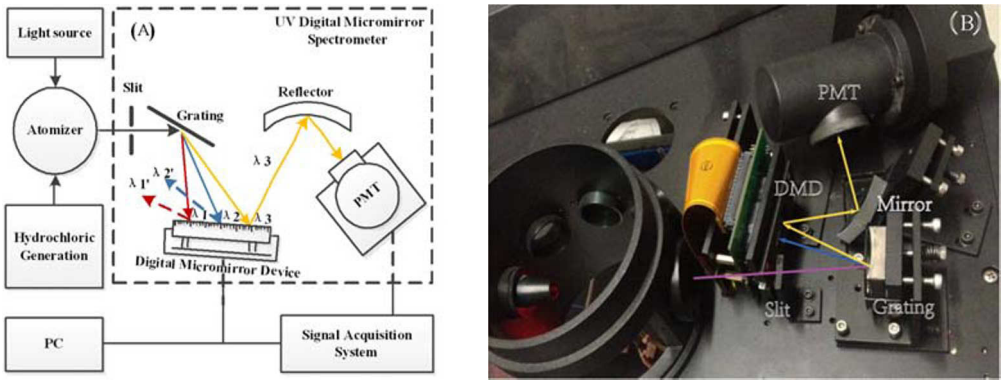

Fig.1 Diagram of UV digital micromirror spectrometer: (A) system structure; (B) physical map

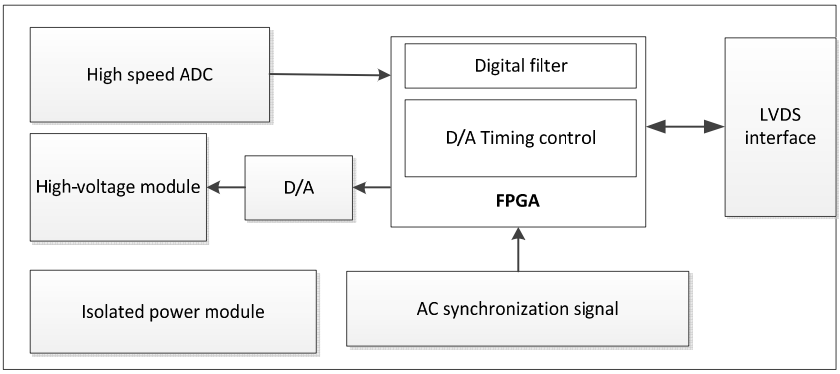

Fig.2 Schematic diagram of dispersion signal acquisition system

3 Experimental

3.1 Experiment platform

A platform consisting of a modified SA-7800 AFS (Beijing Bohui Innovation Optoelectronic Technology Co., Ltd, China) was employed in this experiment, where the non-dispersive detector (PMT) was replaced by the UV digital micromirror spectrometer. As, Sb, Bi and Hg hollow cathode lamps (HCLs, General Research Institute for Nonferrous Metals, Beijing, China) were used as the radiation source, and the detection elements were selected by changing the light source. The reaction condition and experimental platform parameter settings are shown in Table 1.

3.2 Reagents

HCl and NaOH were excellent grade pure; KBH_4 was analytically pure; ultrapure water (impedance > 18 MΩ cm). As, Sb, Bi, Hg standard stock solutions (1000 μg mL^{-1}) were purchased from National Standard Material Center (Beijin), and diluted to a concentration of 2, 4, 8, 10, 20 and 40 μg L^{-1} as As, Sb, Bi, Hg standard series of solutions. A reducing agent solution containing 2.0% (*w/V*) KBH_4, 0.5% (*w/V*) NaOH was additionally prepared.

4 Results and discussion

4.1 Control parameters of DMD

In a complete scanning detection process, the wavelength and intensity of the fluorescent were selected by controlling the rotation of DMD line. The DMD control parameters are shown in Table 2. The wavelength and the DMD line coordinate satisfy the equation: $\lambda = -1.12 \times 10^{-5}N^2 + 0.1755N + 172.67$ (λ means the wavelength and N means the DMD line coordinate). The control principle of DMD is shown in Fig.3A and the schematic of DMD rotating angle is shown in Fig.3B. The scanning range was set to start from line 30 to the end of line 878, which could achieve a spectrum from 180 nm to 320 nm; every rotating action caused the movement of DMD lines backward. The maximum sampling density was obtained when interval line was 1. Since the scanning speed of DMD must be compatible with the pulse timing of HCL and the circuit response time, 100 μs of wait time was required, and it took about 0.848 s (100 μs × 1024 lines) for one spectrum.

Table 1 Setting of experiment platform parameters

Parameters	Setting value
Flow rate of carrier gas	400 mL min^{-1}
Flow rate of shield gas	850 mL min^{-1}
KBH_4 concentration	20 g L^{-1}
HCl concentration	0.5 M
Sample flow rate	0.1 mL s^{-1}
Reductant flow rate	0.05 mL s^{-1}
Atomizer height	8 mm
Lamp primary/boost current of As HCL	60 mA/30 mA
Lamp primary/boost current of Sb HCL	60 mA/30 mA
Lamp primary/boost current of Bi HCL	60 mA/30 mA
Lamp primary of Hg	50 mA
Negative high voltage of PMT	400 V

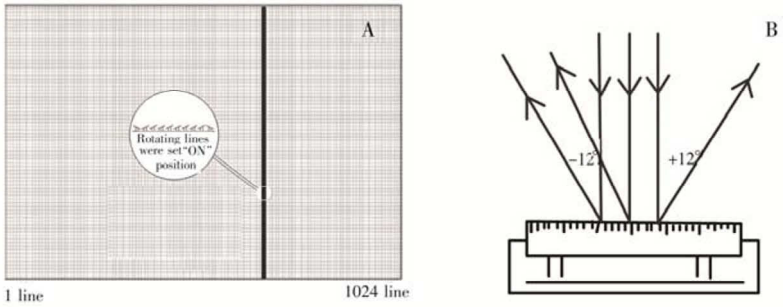

Fig.3 (A) DMD column control flip chart and (B) rotating diagram of DMD

Table 2 Control parameters of DMD

Start line	Final line	Simultaneous rotating lines	Interval lines	Wait time
30th line	878th line	8 lines	1 line	100 μs

4.2 Conditional parameter optimization

4.2.1 DMD simultaneous rollover column number

The lines of digital micromirrors rotated together as an 'exit slit'. It was found that with the increase of the number of simultaneous rotating lines, the fluorescence intensity increased, the full width at half maximum (FWHM) of the peak became wider, and the spectral resolution of UV micromirror spectrometer was affected. Figure 4 shows the relationship between the Hg HCL fluorescence signal intensity at 253.7 nm and the number of simultaneous rotating lines (2–16 columns). When the number of flip columns was 2 column, the measured spectral Full width at half maximum (FWHM) was 2.1 nm, which met the theoretical resolution requirement of spectrometer, but the signal was weak. When the simultaneous rotating lines were set as 16, the measured spectral FWHM was 4.2 nm. However, the minimum distance between the excitation fluorescence peak points of the four elements was 3.6 nm (line of As at 193.7 nm and 197.3 nm). Therefore, it would produce problems such as peak overlap and affected the spectral line analysis. The number of simultaneous rotating lines in the following experiment were set as 8, by which the FWHM was 3.1 nm and met the experimental requirements.

4.2.2 PMT negative high voltage

The fluorescence signal can be effectively converted into photoelectrons and multiplied. Figure 5 shows the alternative relation with the Hg HCL intensity at 253.7 nm and the change of PMT negative high voltage within 220–420 V. The results demonstrated that the fluorescence intensity and the SNR gradually increased with the negative high voltage higher. However, it was limited by the threshold value of PMT high voltage module, and obviously affected by the interference of ambient light and dark current. When the negative voltage was increased over 400 V, the signal strength became weaker and the stability became worse.

4.3 Comparison of transmittance of DMD

The material of the cover window material of commercial UV DMD was Corning 7056 borosilicate glass material[15], which had an inhibitory effect on the transmission of the UV band signal (≤ 280 nm). Meanwhile the cover window material of high UV transmittance DMD was Corning HPFS® 7980 fused silica, which had an effectively increase of the fluorescence signal transmission within 180–280 nm. Figure 6 shows the comparison results between the commercial UV DMD and the high UV transmission DMD with Bi HCL emission lines spectrum as an example. Because the direct signal of the light source was very strong, the acquisition signal was easy to be saturated. The main current of the light source was 30 mA and the negative voltage was 300 V. The fluorescence intensity results were normalized, and the peak intensity of 306.7 nm in Fig.6A was defined as F_m = 1. The experimental parameters for both experiments were same (the lamp primary/boost current was 40/20 mA; negative high voltage of PMT was 280 V). It was found that the commercial UV DMD could hardly transmit below 280 nm. Additionally, the fluorescence intensity achieved by the high UV transmittance DMD had a better performance than that in the case of the commercial UV DMD.

4.4 Emission lines and excitation fluorescence lines

The spectra of the emission fluorescence and excitation fluorescence of standard samples with 0.1 μg mL^{-1} As, 0.1 μg mL^{-1} Sb, 0.1 μg mL^{-1} Bi and 0.1 μg mL^{-1} Hg, respectively, are shown in Fig.7. According to the experimental results and the fluorescence excitation characteristics[19,20], it was shown that

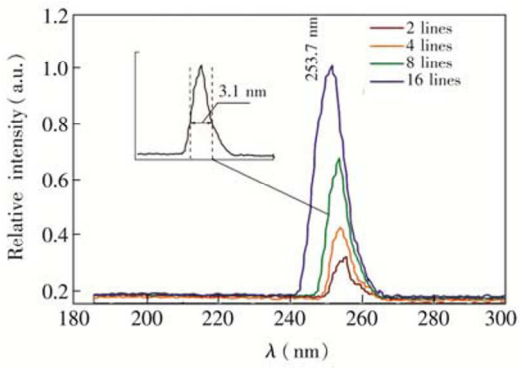

Fig.4 Relationship between simulation rotating lines and fluorescence intensity

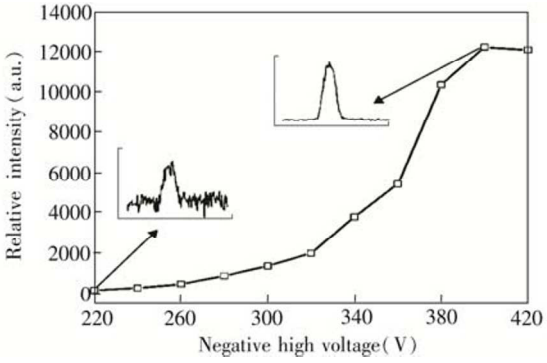

Fig.5 Relationship between negative high voltage of PMT and fluorescence intensity

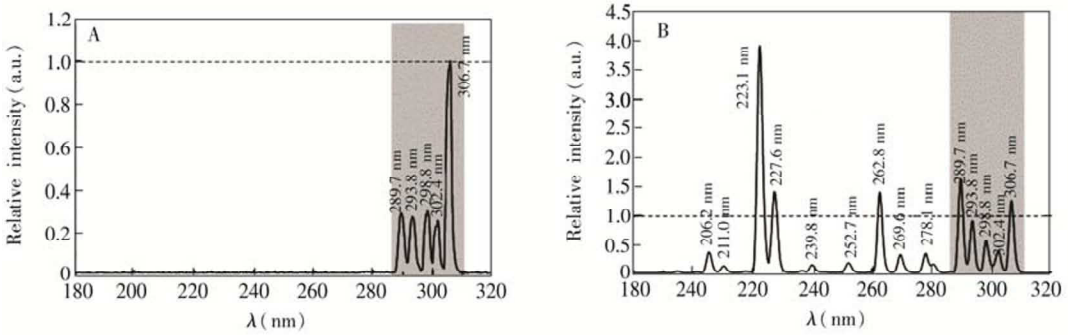

Fig.6 Comparison of transmissions of commercial UV DMD (A) and modified DMD with Corning 7980 Standard Grade fused silica(B). The commercial DMD only has peaks excited in the grey zone, with the dotted line expressing the intensity of the peak at 306.7 nm

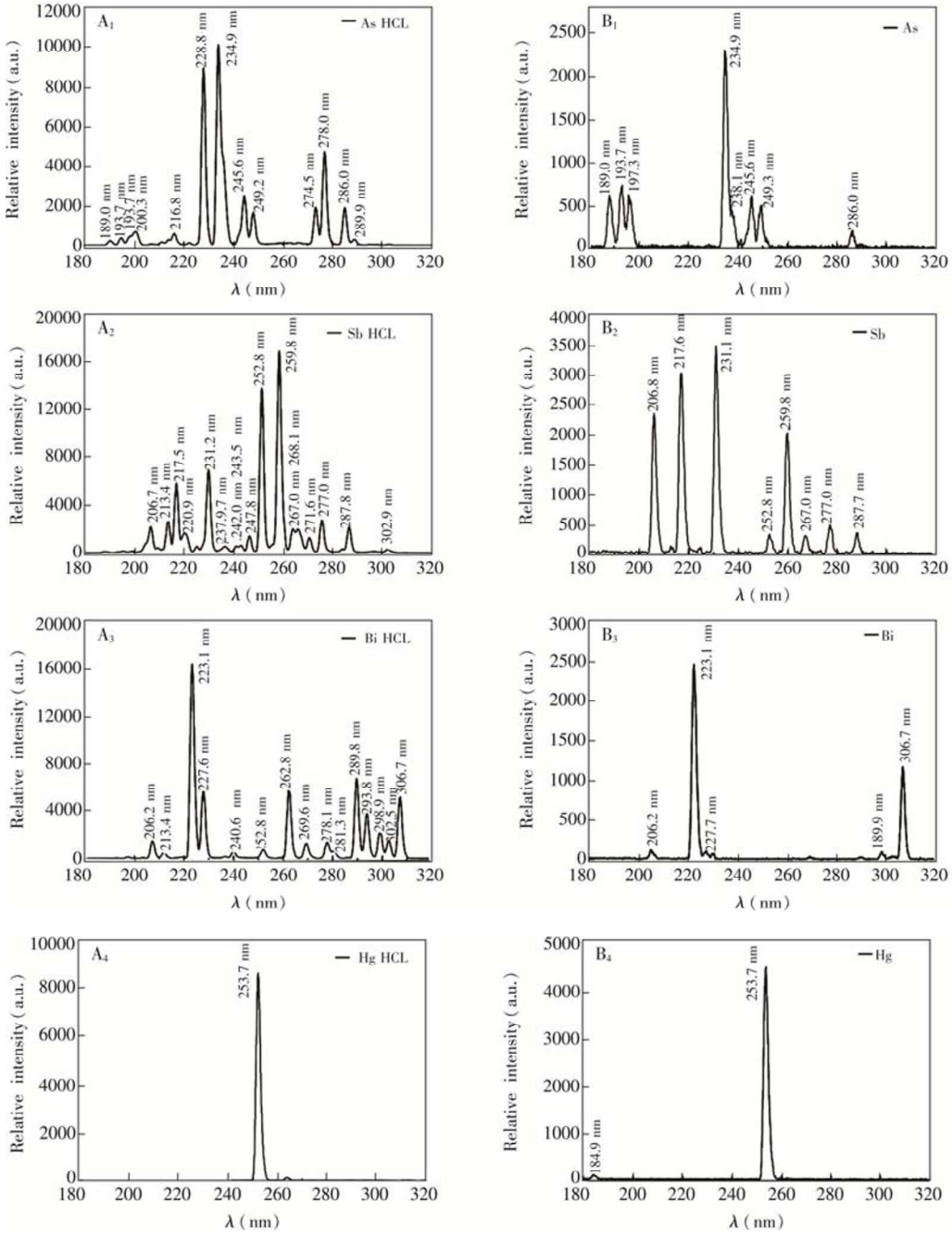

Fig.7 (A) Emission lines spectrum of HCLs of As, Sb, Bi and Hg; (B) Atomic fluorescence spectrum of of As, Sb, Bi and Hg standard sample (0.1 μg mL^{-1})

the resonance fluorescence lines at 189.0, 193.7 and 197.3 nm, and the direct jump fluorescent lines at 234.9, 245.6 and 249.3 nm were observed for As; the resonance fluorescence lines at 206.8, 217.6 and 231.1 nm, and the direct fluorescence lines at 252.8, 259.8, 267.0, 277.0 and 287.7 nm were observed for Sb; the resonance fluorescence lines at 206.2 nm, and the Step fluorescent lines 223.1 and 306.7 nm were observed for Bi; the resonance fluorescence lines at 184.9 and 253.7 nm were observed for Hg. Table 3 summarizes the intensity and proportional relationship between the emission lines of the four elements and the excitation fluorescence.

4.5 Scattering interference effect by light source

The water vapor and small molecular particles in the flame could cause scattering interference in the detection process[21], which may affect the accuracy of the test. In the experiment, Hg element was used as an example to analyze the scattering interference of the light source. The peak at 253.7 nm was found in the blank sample of Hg, as shown in Fig.8A (the purple line). However, the light source was turned off and then the scattering interference peak disappeared, as shown in the black line in Fig.8A. After addition of the Hg standard sample (0.1 μg L^{-1}), a fluorescent signal was obtained as an orange line, as shown in Fig.8A. It was supposed that this phenomenon was caused by HCL scattering interference, and the detected light source scattering interference should be subtracted as background interference, and the real fluorescence signal of Hg standard sample (0.1 μg L^{-1}) was shown as a green line in Fig.8A. The HCL scattering interference experiments of the four elements are shown in Fig.8B. The other scattering interference peaks of As were found at 234.9 nm, Sb at 206.8, 217.6, 231.1 and 259.8 nm, and Bi at 223.1 and 306.7 nm.

4.6 Analysis performances

Table 3 shows the detection limits of standard samples of As, Sb, Bi and Hg at concentration levels of 2, 4, 8, 10, 20 and 40 μg L^{-1}. As shown in Table 3, the detection limit of As was obtained at 234.9 nm with a correlation coefficient of r = 0.9988; Sb at 231.1 nm (r = 0.9989); Bi at 223.1 nm (r =

Table 3 Summary of relationship of important analytical emission and atomic fluorescence lines of As, Sb, Bi, and Hg

Element	Wavelength (nm)	DMD line	Relative emission intensity of light source	Relative fluorescence intensity*	Detection limit* (μg L^{-1})
As	189.0[a]	95th	2.45	30.69	1.04
	193.7[a]	124th	3.83	41.46	0.89
	197.3[a]	145th	7.07	54.40	1.11
	234.9[b]	352th	100.00	100.00	0.23
	245.6[b]	427th	16.48	28.14	1.15
	249.3[b]	447th	24.51	41.89	1.40
Sb	206.8[a]	201th	3.32	64.36	0.59
	217.6[a]	260th	27.23	91.09	0.44
	231.2[a]	339th	34.48	100.00	0.34
	259.8[b]	509th	100.00	55.45	0.66
	277.0[b]	615th	7.38	12.56	3.03
Bi	223.1[c]	292th	100.00	100.00	0.21
	306.7[c]	800th	26.13	49.19	0.58
Hg	253.7[a]	473th	100.00	100.00	0.12

*Excited with high-performance HCL; value corrected for detector spectral response. a. Resonance fluorescence; b. Direct jump fluorescent line; c. Step fluorescence.

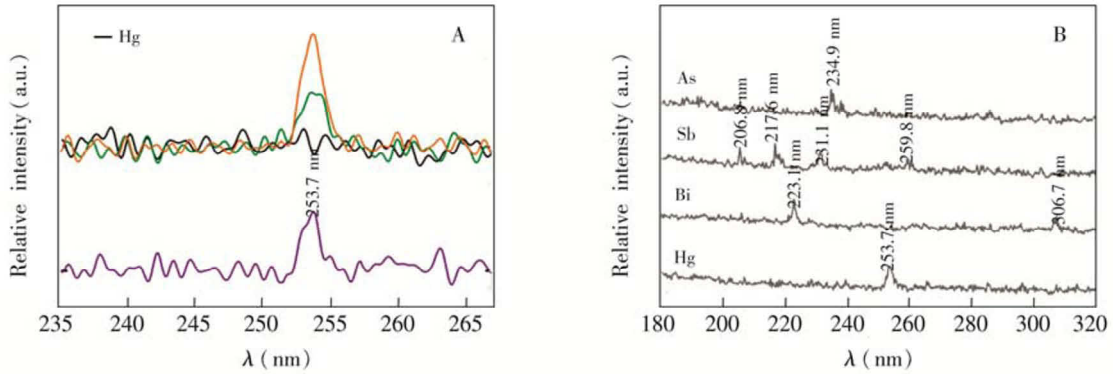

Fig.8 (A) Scattering interference verification experiment of Hg, turning off the light source (black line), fluorescence signal after subtracting the light source scattering interference (green line), fluorescence signal of standard sample at 0.1 μg L^{-1} (orange line); (B) Scattering interference experiments of As, Sb, Bi, Hg

0.9987) and Hg at 253.7 nm (r = 0.9982). The results indicated that the UV DMD spectrometer had the ability of element detection and analysis, but the stability and repeatability of the detection signal need to be further improved. Furthermore, it is necessary to further improve the detection sensitivity of the fluorescence signal. The main components and electrical parts of the UV DMD spectrometer will be integrated in our laboratory to lay the convenience for subsequent performance improvement. The stability test of high UV transmittance DMD and the characteristic of the excitation fluorescence need further research.

5 Conclusions

An atomic fluorescence dispersion detection technique based on DMD was proposed, and an UV digital micromirror spectrometer consisting of high UV transmittance DMD, grating and PMT was developed. The detection ability of As, Sb, Bi and Hg with different characteristic spectral lines was analyzed preliminarily. Furthermore, the scattering interference caused by aerosol and water evaporation during the detection process of blank background was discussed. Compared with the non-dispersive detection method, the UV DMD spectrometer contains no moving parts, and has simple construction and fast analysis speed at 180–320 nm. This work provides a possibility for the study of spectral interference, and also lays a foundation for the application of continuous light source, composite light source or high intensity excitation light source to realize the simultaneous detection of atomic fluorescence multielements. The detection sensitivity of the UV digital micromirror spectrometer needs to be further improved due to the significant attenuation of the fluorescence signal by the spectral structure.

References

[1] Zou Z R, Deng Y J, Hu J, Jiang X M, Hou X D. *Anal. Chim. Acta*, **2018**, 1019: 25–37

[2] Jiang Z G, Zhang J W. *Chinese J. Spectrosc. Lab.*, **2016**, 18(3): 333–336

[3] Gao L, Dong W F, Peng X T, Shi L J, Li Y, Pang Y H. *J. Food Safety Quality*, **2015**, (1): 145–151

[4] Xing Z, Li M. *Anal. Instrument.*, **2017**, (6): 1–15

[5] Yang M, Xue J, Li M, Li J, Huang X, Xing Z. *Anal. Instrument.,* **2012**, 40(8): 1164–1168

[6] Lin H L, Li Z H, Zhu R L, Song B B, Liu P, Bi J P. *Spectrosc. Spect. Anal.*, **2016**, 36(4): 1217–1220

[7] Xu Z, Hu H Y, Chen D K, Cao J X, Yao H. *Anal. Instrument.*, **2015** ,43(4): 490–494

[8] Method A B. 1631: Mercury in Water by Oxidation, Purge and Trap, and Cold Vapor Atomic Fluorescence Spectrometry, **2010**

[9] Norris J D, West T S. *Anal. Chem*., **1973**, 45(2): 5251–5254

[10] Winefordner J D, Elser R C. *Appl. Spectrosc.,* **1971**, 25(3): 345–346

[11] Goueguel C, Laville S, Loudyi H, Chaker M, Sabsabi M, Vidal F, Photonics North. International Society for Optics and Photonics, **2008**

[12] Wagner E P, Smith B W, Madden S, Winefordner J D, Mignardi M. *Appl. Spectrosc*., **1995**, 49(11): 1715–1719

[13] Quyen N T, Jouan M D, Dao N Q, Silva E D, Phuong D A. *Appl. Spectrosc.*, **2008**, 62(3): 273–278

[14] Liu J, Chen F F, Liao C S, Xu Q, Zeng L B. *Spectrosc. Spect. Anal.*, **2011**, 1(10): 2874–2878

[15] Deverse R A, Hammaker R M, Fateley W G. *Vib. Spectrosc.*, **1999**, 19(2): 177–186

[16] Xiang D, Arnold M A. *Applied Spectroscopy*, **2011**, 65(10): 1170

[17] Batchelor J D, Jones B T. *Anal. Chem*., **1998**, 70(23): 4907–4914

[18] Callies B M, Williams R E. US Patent US7161727B2. Filed 2003. Issued **2007**

[19] Dagnall R M, Thompson K C, West T S. *Talanta,* **1967**, 14(12): 1467–1475

[20] Dagnall R M, Thompson K C, West T S. *Talanta*, **1967**, 14(10): 1151–1156

[21] Browner R F. *Analyst,* **1974**, 99: 617–644